J|A|C|S COMMUNICATIONS

Published on Web 04/13/2009

Controlled Formation of an Axially Bonded Co-Phthalocyanine Dimer

Xin Ge,[†] Carlos Manzano,[†] Richard Berndt,*[,†] Lennart T. Anger,[‡] Felix Köhler,[‡] and Rainer Herges*[,‡]

Institute of Experimental and Applied Physics and Otto-Diels-Institute of Organic Chemistry, Christian-Albrechts-University Kiel, 24098 Kiel, Germany

Received January 21, 2009; E-mail: rherges@oc.uni-kiel.de

Large planar π-conjugated compounds are intensively studied as promising materials for applications such as light emitting diodes (OLEDs),[1] organic photovoltaics (OPVs),[2] and organic field effect transistors (OFETs).[3] Particularly metal-phthalocyanines (M-Pcs) are sought after as they are more stable toward light and heat than the commonly used acenes or oligothiophenes and, therefore, hold great promise for practical applications.[4] M-Pcs are already widely used as photoconductors in laser printers, luminescent oxygen sensors, and photovoltaic cells. The decisive parameters for the successful application of organic semiconductors in electronics is the charge mobility, threshold voltage, and on/off current ratio.

These characteristics, in particular the charge mobility, are strongly related to the orbital overlap of adjacent molecules. Therefore, the control of intermolecular interactions in the organic thin films is of utmost importance. Phthalocyanines (Pcs) and metal-phthalocyanines form conducting columnar stacks and herringbone structures in crystals and in thin films which are well investigated.[5] However, very little is known about the electronic nature of the emanating orbital interactions. Ordered single and double layers of Pcs on atomic planar surfaces investigated by STM in combination with theoretical calculations provide a reproducible model system for the investigation of electronic properties of organic thin films that are used in typical applications (e.g., organic thin film transistors). Insight into the electronic nature of the interaction between two PCs in dimeric structures could provide ways to systematically improve the device performance in organic electronics.

Here we use STM to probe and to controllably modify the conductance of a single Co-phthalocyanine (CoPc) molecule (Figure 1) which is located on top of an ordered monolayer on a Cu(111)

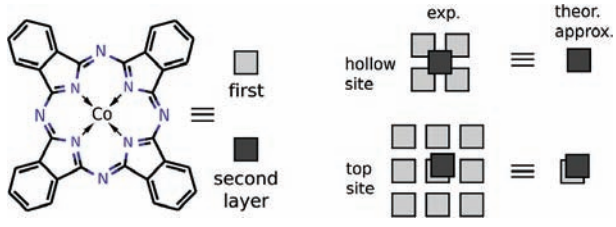

Figure 1. Structure of cobalt-phthalocyanine (CoPc) and schematical respresentation of the theoretical approximation used to model isolated CoPc molecules lying on top of an ordered layer of CoPc on a Cu(111) surface.

single crystal surface. By a minute lateral displacement of the molecule, the formation of a Co−Co bond occurs which manifests itself through a substantially increased conductance at the molecular center. To analyze the experimental results density functional theory (DFT) calculations are used which are enhanced by an empirical dispersion term. We find that unoccupied Co d_{z^2} orbitals interact to form a highly conductive orbital.

[†] Institute of Experimental and Applied Physics.
[‡] Otto-Diels-Institute of Organic Chemistry.

Microscopic aspects of the self-assembly of CoPc on Au(111), Cu(100), and Pb(111) surfaces have been intensely studied with STM.[6−11] Similar to those cases, on the Cu(111) surface used in the present experiment, CoPc appears nearly clover-leaf shaped in STM images and adopts a compact structure (Figure 2). Detailed

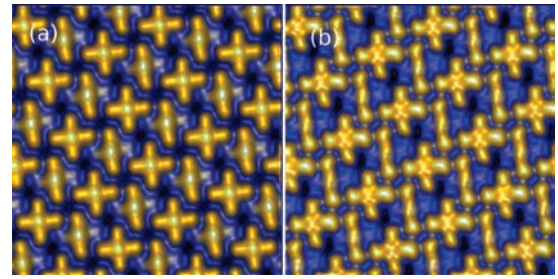

Figure 2. STM image of first layer CoPc on Cu(111). (a) $V = -1$ V and (b) $V = +1$ V, $I = 0.1$ nA, scan size 9×9 nm^2. WSxM[13] was used for image processing.

inspection reveals an additional complication. The symmetry of the molecular orbitals is reduced due to interaction with the C_3-symmetric substrate, and the unit cell comprises two molecules with slightly different adsorption geometries, whose images display an intriguing bias dependence (Figure 2a and b). Wide, well ordered areas are found on the substrate although other phases can be observed, too.[12] Images at negative sample bias V, which are the most sensitive to occupied states, display a protrusion at the molecular center. At positive bias (empty states), the center appears lower than the peripheral benzene rings. Numerical modeling of these contrasts will have to take the metal substrate into account which is beyond the scope of the present study.

While CoPc molecules on top of the first molecular layer tend to aggregate into compact islands some isolated molecules are

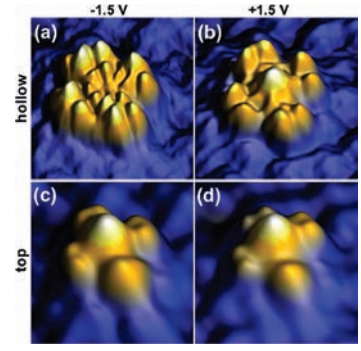

Figure 3. STM images of isolated CoPc adsorbed on the first layer. (a and b) CoPc in "hollow site" position. (c and d) CoPc above a first layer molecule ("top site"). Left column: $V = -1.5$ V corresponding to occupied states. Right column: $V = +1.5$ V, empty states. $I = 0.1$ nA, scan size 3×3 nm^2. At negative bias, the apparent height of a CoPc molecule in the "top" position in the second layer is 0.3 nm.

10.1021/ja900484c CCC: $40.75

observed, too, and exhibit a detailed contrast which is reversed compared to the first layer. In particular, at negative bias (Figure 3a), the structure is resolved at the position of the benzene and pyrrole rings. More importantly, at positive bias (Figure 3b), the conductance of the molecule is largest at the molecular center as reflected by its large apparent height. A similar contrast reversal has been reported by Takada and Tada[13] for CoPc on Au(111). Analysis of the STM images revealed that CoPc molecules which display this bias dependence are located at hollow sites in between four first layer CoPc units. This site, however, does not appear to be the most stable adsorption position for second layer molecules. Often isolated molecules are located almost vertically above a first layer CoPc. These molecules can also be controllably moved from a hollow to a top position by operating the STM at slightly elevated currents ($I = 1$ nA). A typical manipulation sequence is shown in Figure 4. Molecule **A** is moved from its initial hollow position to

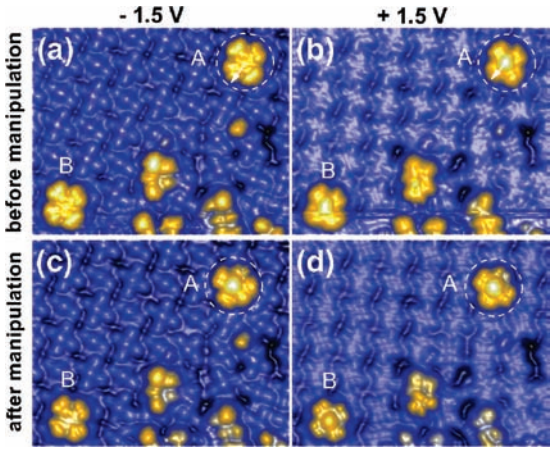

Figure 4. Manipulation of CoPc molecules on the first layer. Initial situation, with molecule **A** and reference molecule **B** located in hollow sites, imaged at (a) $V = -1.5$ V and (b) $V = +1.5$ V. The apparent height of the molecular centers reflecting their conductances is clearly different in (a) and (b). Images, at the same voltages, after manipulation are shown in (c) and (d). Now, molecule **A** is located almost on top of a first layer CoPc. The striking polarity dependence of its image contrast is lost. Reference molecule **B** remains unaffected. $I = 0.1$ nA, scan size 11×9 nm^2.

a top site and concomitantly slightly rotates. Simultaneously, the striking polarity dependence of the conductance of the molecular center vanishes. The center now protrudes independent of the bias polarity (Figure 3c, d). Once adsorbed in a top position, molecules could not be laterally moved with the tip within the parameter range investigated, which indicates more favorable adsorption, although some rotation could be induced. The most striking observation from Figure 3 is the drastically increased conductance of the molecular center of the manipulated molecule, in particular at negative bias.

DFT calculations were used to elucidate the nature of the CoPc−CoPc interaction in the two layers on Cu(111) and to interpret the features in the STM images. All calculations were done using the PBE/TZVP level of DFT including Grimme's dispersion correction method[14] as implemented in the program TurboMole 5.10[15] (for details see Supporting Information). Unfortunately, the computational expenditure to treat the complete system including the metal surface and a large array of molecules at this level of theory is still prohibitive. It was previously shown by Takada and Tada[13] that the electronic structure in the second layer of CoPc is essentially unaffected by the metal surface. We therefore used the CoPc monomer as a computational model for the "hollow site" and the CoPc dimer as a model for the "top site" molecule (Figure 1).

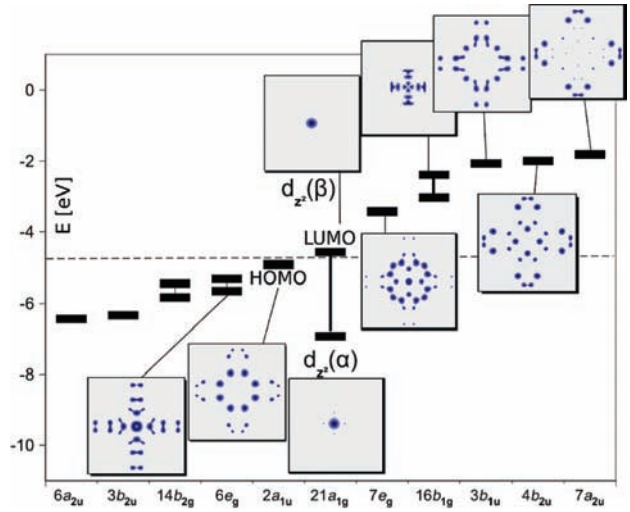

Figure 5. Electron density plots (square of the wave functions) of CoPc. α (spin up) and β (spin down) orbital energy levels are plotted one below the other if they have different energies or on top of each other if they are degenerate. Note that the α and β d_{z^2} orbital energy difference is quite large and only the α d_{z^2} orbital is occupied. The dashed line separates the occupied and unoccupied orbitals.

According to our calculations the HOMO of the isolated CoPc molecule is mainly located at the pyrrol rings of the phthalocyanine unit (8 dots around the center of CoPc, Figure 5). The LUMO is an almost pure d_{z^2} orbital at the Co center (d_{z^2} (β) orbital in Figure 5). Surprisingly, the singly occupied d_{z^2} (α) orbital (Figure 5), responsible for the open shell (doublet) character of the CoPc molecule, is too far below the Fermi level to contribute to the current, which explains the Co center being imaged as a depression at negative bias (Figure 3a).

To elucidate the electronic structure of the CoPc dimer as a model for the top site arrangement (Figure 1) we extensively scanned the potential energy hypersurface of two CoPc units in different orientations (for details see Supporting Information). The most stable dimer **b3** (dimerization energy 37.6 kcal/mol) indeed is the one which fits most closely to the orientation found in the STM picture for the "top site". The two CoPc units are lying parallel with respect to each other at a distance of 2.868 Å. A slight parallel translation of 1.005 Å results in a Co−Co distance of 3.039 Å. This distance is considerably shorter than that in a nonbonding interaction although it exceeds the value expected for a two-electron σ type Co−Co bond (~2.8 Å).

Close inspection of the Kohn−Sham molecular orbitals (Figures 6, 7) reveals a strong interaction between the empty $d_{z^2}(\beta)$ orbitals

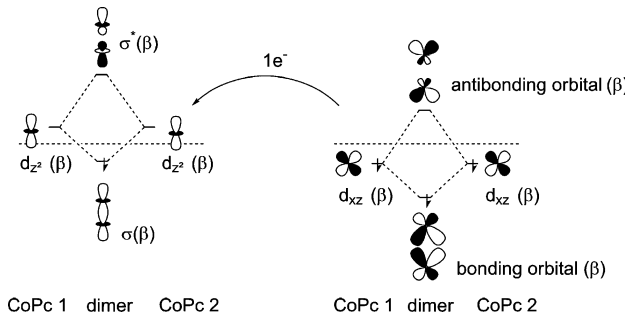

Figure 6. Molecular orbital interaction diagram of two unoccupied d_{z^2} orbitals (left) and two occupied d_{xz} orbitals (right) of two separate CoPc molecules upon approaching each other in C_{2h} symmetry. The dashed line separates the occupied and unoccupied orbitals.

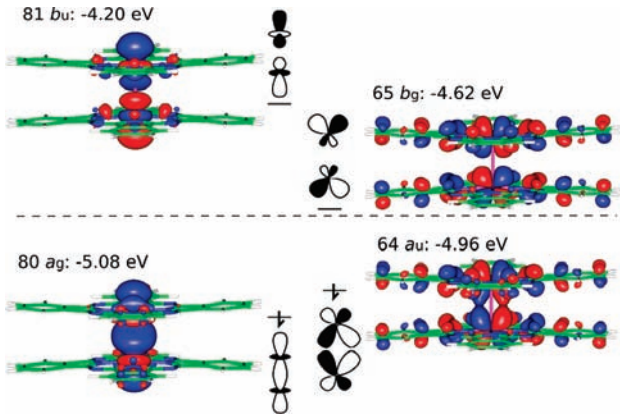

Figure 7. Singly occupied molecular orbitals involved in the bonding interaction between two CoPc molecules in the most stable dimer structure (below dashed line) and the corresponding unoccupied orbitals (above dashed line). The line of sight is parallel to the lateral displacement of the two CoPc units.

of the two CoPc molecules. The two initially empty $d_{z^2}(\beta)$ orbitals form a lower energy bonding and a higher energy antibonding combination (σ and σ^*). The interaction is strong enough to shift the bonding combination into the region of occupied molecular orbitals. In the CoPc dimer (top site) this high lying occupied $d_{z^2}(\beta)-d_{z^2}(\beta)$ σ-bonding orbital is occupied by one electron and causes the bright spot in the middle of the CoPc structure in the STM at negative bias. The antibonding combination (σ^*) remains empty and gives rise to the bright spot at positive bias. Therefore, unlike in the isolated CoPc (hollow site), the CoPc dimer (top site) exhibits a high conductance at the center of the molecule at negative as well as at positive bias.

A similar orbital interaction occurs with the $d_{xz}(\beta)$ orbitals of the Co atoms, which are occupied in the isolated CoPc. Upon forming the dimer they split into a bonding/antibonding combination. The antibonding state is shifted into the region of unoccupied orbitals, resulting in a net transfer of an electron into the bonding combination of the $d_{z^2}(\beta)$ orbitals. Consequently, there are two unpaired electrons in the CoPc dimer (triplet state), which are located in a σ type bonding $d_{z^2}-d_{z^2}$ orbital between the Co atoms and in the bonding combination of two d_{xz} orbitals.

This MO scheme also explains why no highly symmetric D_{4h} structure (two CoPc's exactly on top of each other) was found. In our calculations, in the STM experiments, as well as in X-ray and neutron diffraction structures of CoPc[16,17] and of similar systems,[18] the two CoPc units are always shifted toward C_{2h} symmetry. In D_{4h} symmetry the d_{xz} and d_{yz} orbitals in CoPc are degenerate and so are the bonding and antibonding MOs resulting from their interaction upon dimer formation. The electron which is needed to occupy the new bonding $d_{z^2}-d_{z^2}$ combination can be transferred from either the bonding $d_{xz}-d_{xz}$ or the $d_{yz}-d_{yz}$ combination which leads to Jahn−Teller distortion toward C_{2h} symmetry. A similar parallel displaced geometry was theoretically predicted for the parent porphine dimer.[19]

We also addressed the possibility of a spin crossover from a triplet state of the dimer to a singlet state. There is precedence in Co(II) chemistry. $[Co(CN)_5]^{3-}$ is paramagnetic and the dimer $K_6[Co_2(CN)_{10}]$ is diamagnetic. According to an X-ray structure of the barium salt the Co−Co distance is 2.794 Å.[20,21] No similar singlet structure of the CoPc dimer was found. Spin pairing of the two doublet monomers to form a short Co−Co bond is probably hindered by the rigid CoPc framework, which would have to bend considerably out of planarity to get the two Co atoms close enough to each other for spin pairing.

In summary, we have used STM to laterally move single CoPc molecules on an ordered molecular layer of CoPc. An increased binding interaction was observed if the CoPc in the second layer is placed almost on top of the CoPc underneath. DFT calculations show that an unusual axial Co−Co bond is formed from the d_{z^2} and d_{xz} orbitals, which also explains why a perfect symmetrical stacking arrangement is unfavorable. This orbital interaction leads to a substantial increase of the conductance of the molecular center at negative bias and provides an explanation for the conductance along the columnar stacks of CoPc in thin films. Our results also demonstrate that STM in combination with DFT can be used as a powerful tool to elucidate the nature of unusual chemical bonding modes.

Acknowledgment. The authors thank Jorge Cerda and Hao Tang for discussions. Financial support from the Deutsche Forschungsgemeinschaft via SFB 677 is gratefully acknowledged.

Supporting Information Available: Computational and experimental details. This material is available free of charge via the Internet at http://pubs.acs.org.

References

(1) Baldo, M. A.; O'Brien, D. F.; You, Y.; Shoustikov, A.; Sibley, S.; Thompson, M. E.; Forrest, S. R. *Nature (London)* **1998**, *395*, 151–154.
(2) Martinson, A. B. F.; Massari, A. M.; Lee, S. J.; Gurney, R. W.; Splan, K. E.; Hupp, J. T.; Nguyen, S. T. *J. Electrochem. Soc.* **2006**, *153*, A527–532.
(3) Che, C.-M.; Xiang, H.-F.; Chui, S. S.-Y.; Xu, Z.-X.; Roy, V. A. L.; Yan, J. J.; Fu, W.-F.; Lai, P. T.; Williams, I. D. *Chem. Asian J.* **2008**, *3*, 1092–1103.
(4) Yamada, H.; Okujima, T.; Ono, N. *Chem. Commun.* **2008**, 2957–2974.
(5) Gould, R. D. *Coord. Chem. Rev.* **1996**, *156*, 237–274.
(6) Lu, X.; Hipps, K.; Wang, X.; Mazur, U. *J. Am. Chem. Soc.* **1996**, *118* (30), 7197–7202.
(7) Suto, K.; Yoshimoto, S.; Itaya, K. *J. Am. Chem. Soc.* **2003**, *125* (49), 14976–14977.
(8) Takada, M.; Tada, H. *Chem. Phys. Lett.* **2004**, *392* (1−3), 265–269.
(9) Zhao, A.; Li, Q.; Chen, L.; Xiang, H.; Wang, W.; Pan, S.; Wang, B.; Xiao, X.; Yang, J.; Hou, J. G.; Zhu, Q. *Science* **2005**, *309* (5740), 1542–1544.
(10) Jiang, P.; Ma, X.; Ning, Y.; Song, C.; Chen, X.; Jia, J.-F.; Xue., Q.-K. *J. Am. Chem. Soc.* **2008**, *130* (25), 7790–7791.
(11) Katano, S.; Kim, Y.; Hori, M.; Trenary, M.; Kawai, M. *Science* **2007**, *316* (5833), 1883–1886.
(12) Ge, X. Dissertation, Mathematisch-Naturwissenschaftliche Fakultät, University of Kiel, Germany, 2006.
(13) Horcas, I.; Fernández, R.; Gómez-Rodríguez, J. M.; Colchero, J.; Gómez-Herrero, J.; Baro, A. M. *Rev. Sci. Instrum.* **2007**, *78* (1), 013705.
(14) Grimme, S. *J. Comput. Chem.* **2006**, *27* (15), 1787–1799.
(15) Ahlrichs, R.; Bär, M.; Häser, M.; Horn, H.; Kölmel, C. *Chem. Phys. Lett.* **1989**, *162* (3), 165–169.
(16) Mason, R.; Williams, G. A.; Fielding, P. E. *Dalton Trans.* **1979**, 676–683.
(17) Williams, G. A.; Figgis, B. N.; Mason, R.; Mason, S. A.; Fielding, P. E. *Dalton Trans.* **1980**, 1688–1692.
(18) Olmstead, M.; Costa, D.; Maitra, K.; Noll, B.; Phillips, S.; Van Calcar, P.; Balch, A. *J. Am. Chem. Soc.* **1999**, *121* (30), 7090–7097.
(19) Mück-Lichtenfeld, C.; Grimme, S. *Mol. Phys.* **2007**, *105*, 2793–2798.
(20) Simon, G. L.; Adamson, A. W.; Dahl, L. F. *J. Am. Chem. Soc.* **1972**, *94* (22), 7654–7663.
(21) Brown, L. D.; Raymond, K. N.; Goldberg, S. Z. *J. Am. Chem. Soc.* **1972**, *94* (22), 7664–7674.

JA900484C